# Defining B Cell Immunodominance to Viruses

**Davide Angeletti**[1], **James S. Gibbs**[1], **Matthew Angel**[1], **Ivan Kosik**[1], **Heather D. Hickman**[1], **Gregory M. Frank**[1], **Suman R. Das**[1,2], **Adam K. Wheatley**[3], **Madhu Prabhakaran**[3], **David J Leggat**[3], **Adrian B. McDermott**[3], and **Jonathan W. Yewdell**[1]

[1]Laboratory of Viral Diseases, National Institutes of Allergy and Infectious Diseases, National Institutes of Health, Bethesda MD

[2]Department of Microbiology, Vanderbilt University, Nashville, TN

[3]Vaccine Research Center, National Institutes of Allergy and Infectious Diseases, National Institutes of Health, Bethesda MD

## Abstract

Immunodominance defines the hierarchical immune response to competing antigens in complex immunogens. Little is known regarding B cell and antibody immunodominance despite its importance to immunity to viruses and other pathogens. We show that B cells and serum antibodies from inbred mice demonstrate a reproducible immunodominance hierarchy to the five major antigenic sites in the influenza A virus hemagglutinin globular domain. The hierarchy changes as the immune response progresses and depending on antigen formulation and delivery. Passive antibody transfer and sequential infection experiments demonstrate "original antigenic suppression", where antibodies suppress memory responses to the priming antigenic site. Our study provides a template for attaining deeper understanding of antibody immunodominance to viruses and other immunogens.

Immunodominance (ID) is the complex phenomenon of unequal immunogenicity between different immunogens and different epitopes on the same immunogen. While there is reasonably good understanding of CD8^{+} T cell ID[1], far less is known about B cell and antibody (Ab) ID. Indeed, the promise of "universal vaccines" for antigenically variable viruses such as HIV and influenza A virus (IAV) based on targeting conserved regions of viral proteins[2,3], in large part depends on circumventing the immune system's marked tendency to focus on variable epitopes[4,5].

IAV is a relatively complex antigen. Virions contain at least 10 viral gene products[6], and infected cells express at least 5 additional gene products that are potentially immunogenic in virus-infected hosts. Of these, hemagglutinin (HA) is of prime importance for vaccines. Only Abs to HA efficiently prevent infection, which is achieved by blocking HA-mediated attachment to the cell surface or HA-mediated fusion of viral and host cell membranes[7]. Although other viral proteins are more abundant in virions, HA is immunodominant in serum Ab responses to virions in mammals, birds, and remarkably, even lamprey, despite the enormous structural difference between Abs of jawed vertebrates versus lamprey[8]. Intense interest in HA immunogenicity is based on the importance of antigenic drift in HA, necessitating annual re-vaccination with ever-updated IAV strains.

Classical studies with monoclonal Ab escape mutants defined five overlapping antigenic sites in the globular domain of the PR8 (H1) HA as the major target of virus-neutralizing Abs[9–11]. Sa and Sb sites are located on the tip of the globular head of the homotrimeric molecule, while Ca1, Ca2 and Cb sites are located towards the stem structure that supports the head and attaches the HA to the membrane. Pioneering studies examined the anti-HA Ab ID hierarchy using anti-HA B cell hybridomas generated from IAV immunized BALB/c mice. These revealed the early predominance of Cb-specific hybridomas, followed by a prevalence of Sb-specific hybridomas after secondary immunization[12–14]. As the work was limited to hybridomas, it remains uncertain how representative the findings are for B cells and serum Abs. Here, we generated a panel of Ab-selected IAV escape mutants. This tool allowed us to dissect B cell and polyclonal Ab ID at the level of individual antigenic sites.

## RESULTS

### 4 viruses preserve one intact antigenic site

The PR8 HA has five overlapping antigenic sites on its globular head that are targets of the large majority of the Ab response (Fig. 1a)[8–10,15]. To investigate immunodominance in B cell responses we generated a panel of viruses with multiple mutations that would enable facile determination of B cell and serum Ab specificity. The goal was to produce five " 4" viruses: viruses that maintain one antigenic site identical to the parental virus while antigenically altering the other four.

We initially employed panels of selecting mAbs to determine the minimal number of mutations required to abrogate the antigenicity of each antigenic site. Using this information, we attempted, but ultimately failed, to directly genetically engineer the ideal panel of viruses to maintain a consistent sequence at each of the mutated sites in the 4 virus panel. This failure echoes our previous observations in generating a complete globular domain escape virus by 12 sequential individual mAb selection steps (we refer to this virus as S12)[15].

Consequently, we used mixtures of mAbs specific for a common antigenic site in an iterative sequential process. After multiple rounds of mAb selection, we obtained a panel of viruses that shared common mutations for Sb (with one exception), Ca1, Ca2, and Cb sites, but with unique mutations for the Sa site (Supplementary Table 1). For Sb, Ca1 and Ca2 sites, a single amino acid substitution was sufficient to ablate the binding of a large fraction of

representative site-specific mAbs. By contrast, the Sa and Cb sites required 3 and 4 mutations, respectively.

To define the antigenicity of these viruses in detail, we used a panel 62 well-characterized mAbs specific for the known antigenic sites in ELISAs (Fig. 1b)[10,15]. The results showed that the Sa, Sb, and Cb   4 viruses largely maintained the cognate antigenic site while demonstrating greatly reduced affinity with nearly all mAbs specific for the altered sites. Not surprisingly, given their intimate physical relationship, it proved most difficult to completely separate Ca1 and Ca2   4 viruses in the Ca sites.

We further validated the predicted specificity of the   4 panel using polyclonal guinea pig (GP) serum raised to PR8. We depleted GP serum with either wild-type PR8, each of the   4 viruses, S12, or as a negative control, an influenza B virus (IBV). We then generated Fab-fragments from five representative mAbs (one per antigenic site) and used the depleted sera to compete for their binding in ELISA. Absorbing GP sera with either S12 or IBV failed to remove Abs that could compete with any of the Fabs examined (Supplementary Fig. 1a). As expected, the positive control of absorbing with PR8 removed nearly all competing Abs for each of the Fabs, except the Ca2 Fab. Absorption with each of the   4 viruses selectively removed Abs that competed with the cognate Fab. Interestingly, for Ca2 and Ca1 sites, absorption with the cognate   4 virus actually *increased* the binding of the cognate Fabs. This is explained by previous findings where binding of Sa-specific Abs enhances the binding of Ca-specific Abs[16]. Thus, in the absence of competing Ca-specific Abs the remaining Sa-specific Abs enhanced Fab binding, extending the enhancement phenomenon to serum Abs.

Based on these findings we conclude that the antigenic sites in the   4 virus panel are sufficiently well resolved to use the panel to characterize B cell and Ab immunodominance.

## B cell ID hierarchy is dynamic and well ordered

We next used the   4 virus panel to investigate immunodominance in B cell responses in mice infected intranasally (i.n.) with PR8. Extrafollicular B cells respond rapidly to IAV in draining mediastinal lymph nodes (MLN)[17–19]. We first measured responses using ELISPOT to enumerate Ab-secreting cells (ASCs) at various days post-infection (p.i.). We used   4-recombinant HA (rHA) as ELISPOT probes to determine site specificity of the response. Immediately responding ASCs are most likely short-lived plasma cells that comprise the immediate helper T cell and germinal center (GC)-independent response[18,19]. By d 14 ASCs are mostly derived from early diversified and affinity-matured GC B cells[20].

ELISPOT analysis of MLN shows the expected rapid increase of ASCs between d 3 and 7 (Fig. 2a). Cb-specific B cells dominate the early response, consistent with early findings using hybridomas[12]. Low numbers of B cells specific for each of the other sites are detected at d 7 but not on d 9, then recover, with Sb-specific ASCs outnumbering ASCs specific for Sa, Ca1 or Ca2.

By two weeks p.i. humoral responses are dominated by rapidly dividing GC-derived B cells, which, in addition to their numerical advantage versus extrafollicular B cells, secrete

affinity-matured Abs. Unlike plasma cells, GC B cells have appreciable amounts of cell surface Ig, enabling their flow cytometric characterization using fluorescently labeled antigens (Supplementary Fig. 2a).

We quantitated GC B cells using rHA probes based on our 4 viruses with an additional mutation in the sialic binding site (Y98F) to abolish HA binding to cell-surface sialic acids (Supplementary Fig. 2b)[21]. Each of the rHA probes bound to GC B cells from mice infected with PR8 (positive control) but not J1, a reassortant PR8 virus containing just the H3 HA gene segment (negative control), demonstrating their specificity (Supplementary Fig. 2c).

Analyzing MLN GC B cells of PR8-infected mice at 14, 21, and 28 d.p.i., we found that Cb-specific B cells dominate on d 14 and 21 (Fig. 2b). On d 14, only Sa-specific B cells were significantly above frequencies observed using S12 rHA, which we use to set background frequencies for identifying globular domain–specific B cells. By d 28, numbers of B cells specific for each of the 4 other sites approached Cb-specific B cell numbers. The sum of each of the specificities on each day was similar to the total HA response measured using wild-type PR8 HA to stain cells (Supplementary Fig. 2d), supporting the validity of using the 4 virus panel to quantitate immunodominance.

These findings show that Cb responses rapidly emerge in both extrafollicular and GC B cells. Upon several rounds of affinity maturation and GC selection, the GC response becomes more diversified with broader specificity.

## ID of serum Abs is dynamic and correlates with GC B cells

We previously reported that the average affinity of GC B cells for HA predicts the affinity of the anti-HA serum Ab response[22]. To examine how the specificity of anti-HA GC B cells predicts serum response, we measured site-specific serum polyclonal Ab (pAb) responses via ELISA using purified HA from wild-type and 4 viruses as antigens and anti-$\kappa$ chain secondary Ab to detect both IgG and IgM. Binding to S12 HA defines the background of non-canonical anti-globular domain and anti-stem Abs binding to a nearly completely drifted HA globular domain. Anti-HA titers increased 2.5-fold between d 14 and 40 post i.n. infection (Fig. 2c). Consistent with our quantitation of ASCs and GC B cells, Cb-specific Abs rose quickly after infection, attaining near maximum titers by 14 d.p.i. We barely detected Abs specific for other sites on d 14. Of these, Sb-specific Abs were the first to increase, nearly reaching Cb-specific Ab titers one week later, and then surpassing Cb-specific Ab titers after another week, and maintaining immunodominance at d 40. Sa-and Ca2-specific Abs were first detected on d 28, and continued to increase on d 40. Ca1-specific Abs were only detected above background values on d 40. The cumulative response towards the 5 antigenic sites was close to the response to wild-type PR8, further corroborating our ability to dissect ID with the 4 virus panel (Fig. 2d). We did not detect antigenic site specific-differences in isotype composition of Abs, with IgM constituting 25% of the Abs at d 14 and progressively waning thereafter (Supplementary Fig. 3).

While B cells specific for Sa- and Sb-sites were, respectively, higher and lower at earlier times as compared to serum Abs, in general, we measured a strong positive correlation between frequency of antigen-specific GC B-cells and serum Abs (Fig. 2e). Thus, as with

Ab affinity[22], numbers of follicular GC B cells in the draining LN accurately predict subsequent serum response, likely because LN GC B cells are the primary source of Ab once they become ASCs after migrating from immune organs.

Parallel analysis performed on splenic GC B cells showed that overall immunodominance pattern was similar, particularly on d 14, when Cb-specific B cells were highly dominant (all other specificities were at S12 background values) (Supplementary Fig. 4a). At later days, however, the pattern was clearly distinct from the MLN, with Sa-specific B cells moving up in the hierarchy with other specificities. Most importantly, there was a poor correlation between the splenic GC B cell immunodominance hierarchy and serum Ab responses (Supplementary Fig. 4b), suggesting that most Abs arise from B cells originating in proximal LNs.

When considering total number of HA-binding GC B cells rather than frequency, we observe the same phenomenon, with strong positive correlation of serum Abs with MLN cell numbers but not splenic cell numbers (Supplementary Fig. 4c,d). Importantly, the total number of rHA-binding cells (Spleen + MLN) also correlated well with serum Abs (Supplementary Fig. 4e). Taken together, these data strongly imply that B cells originating in the draining LN GCs are the prinicpal source of serum Abs.

## Vaccination alters the immunodominance hierarchy

A critical practical question is how vaccination and infection differ in eliciting protective immunity. We immunized mice once via intramuscular (i.m.) or intraperitoneal (i.p.) injection with purified PR8 that we had UV-irradiated sufficiently to reduce *de novo* synthesis of viral proteins in infected cultured cells to undetectable levels. We co-formulated virus injected i.m. with Titermax Gold adjuvant. We then measured site-specific serum Abs and MLN and splenic GC B cells on d 14 and 28 post-immunization.

Intraperitoneal immunization gave a more rapid response, with i.m. immunization yielding low serum Ab titers on d 14 (Fig. 3a,b). At d 28, i.p. titers were unchanged, while i.m. titers increased to nearly match i.p. induced Abs. Notably, the d 28 serum Ab response to vaccination was actually greater than the response following i.n. infection. While all three responses were of similar magnitude, there were striking differences in the immunodominance hierarchy.

With vaccination-elicited Abs, we did not observe the highly dynamic changes in the immunodominance hierarchy we observed following infection. Further, the majority Abs targeted the Sa and/or Sb antigenic sites at both d 14 and d 28, but not the Cb site. Measuring the frequency of splenic GC cells specific for each antigenic site 14 or 28 d post i.p. injection reveals a strong correlation between GC frequency and the serum response (Fig. 3c), suggesting that splenic B cells are a major sources of serum Abs following i.p. injection. The correlation for Sa- and Sb-specific B cells was not as robust, suggesting that these B cells might be preferentially generating rapidly proliferating, short-lived ASCs. Peritoneal lymph is reported to drain largely to the MLNs[23], but our data suggests that some peritoneal antigens may equally well traffic to the spleen. Indeed, analysis of MLN at 14

d.p.i. shows a near perfect correlation between splenic and MLN GC B cell frequencies (Supplementary Fig. 3f).

Taken together these findings clearly show that the immunodominance hierarchy is greatly influenced by the form and route of antigen and is not rigidly dictated by a uniform lymphoid B cell repertoire.

## CD4+ T cells do not influence immunodominance

To study the influence of CD4+ T cell-mediated help on the anti-HA immunodominance Ab hierarchy, we challenged CD4-depleted mice by i.n. infection or i.p. immunization (Fig. 4). As reported previously[24,25], we found that CD4+ T cells were necessary for high and sustained anti-HA serum Ab titers (Fig. 4). Indeed, at d 28, we barely detected serum anti-HA Abs after i.n. infection. While serum Ab responses were more durable after i.p. immunization, titers diminished and did not increase as when CD4+ T cells were present (Fig. 4a). Following either infection or immunization, T cell depletion prevented GC formation as determined by the absence of B cells with GC markers by both flow cytometry and immunofluorescence of frozen MLN (infection) or spleen sections (immunization) (Supplementary Fig. 5).

Despite ablating GCs and compromising serum Ab responses, depleting CD4+ T cells had remarkably little effect on the immunodominance hierarchy following i.n. infection or i.p. immunization (Fig. 4a,b). Plotting the untreated versus CD4+ T cell depleted responses against each other revealed an excellent correlation. CD4+ T cell depletion had a greater impact on ID following i.p. immunization, particularly on d 14 where Sa dominated and Sb was diminished. However, the overall correlation with non-depleted serum Abs was still robust (Fig. 4c). These findings show that while CD4+ T cell help is necessary for high and durable Abs titers, it is not a key modulator of the immunodominance hierarchy.

## Stem-specific Abs are present at low titers

To measure the fraction of serum Abs specific for the conserved stem-region of HA we used a chimeric virus with an antigenically shifted head (H5) and the PR8 stem[26] and examined nearly all sera described above by ELISA (Supplementary Table 2). As expected, after a single i.n. infection stem specific serum Abs were detectable only at low titers, and interestingly, did not increase with time. Similarly, neither i.p. or i.m. immunization generated robust anti-stem responses, though in both cases titers increased with time, and the early response to i.m. immunization, while weak, represents a significant fraction of the globular domain response. CD4+ T cell depletion slightly decreased anti-stem Ab responses. Stem responses were modestly increased by boosting i.p. after i.n. immunization. Thus, as expected, stem-specific Ab responses are not strongly induced in primary immune responses, or after a single challenge immunization.

## Mouse genetic background influences ID

To examine the extent to which C57BL/6 and BALB/c mice differ in their B immunodominance hierarchies, we examined serum Abs in BALB/c mice d 14 and 28 d following i.n. infection or i.p. immunization (Fig. 5a, b). The anti-Cb Ab response to i.n.

infection was of similar magnitude in BALB/c and C57BL/6 mice on d 14 and 28, however it descended one rung on the immunodominance hierarchy, due to the ascension of Sb-specific Abs, which were dominant on both days. Further, the early Sa-specific Ab response was much more robust, and even surpassed the Cb-specific response on d 28. Ca2 Abs also showed slightly higher responses at 14 d than in C57BL/6 mice, where they were not detected above background values (Fig. 5c). Upon i.p. immunization, Sa and Sb-specific Abs dominated from the initial time points and the pattern did not change after 28 d, similar to C57BL/6 mice (Fig. 5d). Thus, there are differences in the immunodominance hierarchies in BALB/c and C57BL/6, particularly in the early response following i.n. infection.

### Polyclonal Abs show antigenic site-specific functions

Our findings show that there is a highly reproducible and dynamic HA antigenic site-specific immunodominance hierarchy in Ab responses following IAV infection or vaccination. To understand the functional consequences of differential responses to the antigenic sites, we infected mice with each Δ4 virus and collected sera on d 21 for testing in ELISA, hemagglutination inhibition (HI) and virus neutralization (VN) assays. Normalizing each activity to the ELISA area under the curve (AUC) titer, we could assess the specific antiviral activity of pAbs for each antigenic site.

As predicted from previous unpublished studies with mAbs (Supplementary Table 3), Cb-specific pAbs exhibited the lowest specific activities in HI and VN assays while Sa-specific pAbs exhibited high specific activities in both assays (Fig. 6a,b). Sb-specific pAbs demonstrated high activity in VN, as previously observed for Sb-mAbs. Unexpectedly, however, in HI assays the specific activity of Sb-specific pAbs was even lower than Cb-specific pAbs (Fig. 6a).

To investigate whether Ab avidity could explain the site-dependent functional differences we used our newly developed method that allows determination of average B cell population avidity[22]. This "$AC_{50}$ method" is based on graded flow cytometric staining of GC B cells with fluorescent rHA to calculate the $AC_{50}$ value, the concentration of rHA that stains 50% of GC B cells, which closely tracks the affinity of serum Abs[22].

We used wild-type PR8 rHA to stain GC cells from mice infected with each of the Δ4 viruses (Fig. 6c). A large fraction of PR8 binding-Abs in these mice are specific for the preserved antigenic site (Supplementary Fig. 6). $AC_{50}$ measurements revealed that B cells specific for each of the sites generated Abs with high average affinity, ranging from 1.4 nM to 4 nM (Fig. 6d). These findings demonstrate that there can be small but significant differences in Ab affinity at the level of antigenic sites. This difference does not, however, account for the site-specific functional differences in pAbs in VN and HI assays. While Cb-specific GC B cells have the highest average affinity, Cb-specific pAbs have the lowest functional activities. Thus, the site-specific functional differences are likely to be due to the location of the sites and not to the affinities of Abs elicited.

### Modulating immune responses

A critical complexity of human influenza vaccination is the effect of pre-existing Abs on subsequent responses. With the exception of young children, virtually everyone vaccinated

with IAV has been previously infected and/or vaccinated with IAV. To examine the influence of competing Abs on vaccination, we vaccinated mice i.p. with UV inactivated PR8 mixed with high affinity Fab fragment ($K_D$=45nM) of the H28-E23 Sb-specific mAb. We used a Fab fragment to avoid potential complications of altering antigen presentation/processing due to Fc mediated uptake or association with complement and other serum proteins.

Including H28-E23 Fab in the vaccine decreased the overall anti-HA response on both d 14 and 28 by ~ 5-fold (Fig. 7a). Remarkably, while the Sb response was almost completely suppressed, the immunodominance hierarchy otherwise was similar on both days (Fig. 7a,b). Since the Sb response is normally dominant on d 28, this indicates that Sb B cells do not "immunodominate" other specificities, as is often observed in CD8^{+} T cell responses[27,28].

To extend these findings to a more physiological setting, we infected mice i.n. with either Sb 4 or Cb 4 and 28 d later challenged via i.p. vaccination with UV inactivated wild-type PR8. We chose these viruses since their cognate preserved sites are immunodominant on d 28. Seven days post-challenge, we measured the immunodominance hierarchy among serum Abs via ELISA (Supplementary Fig. 7).

The results partially recapitulated the Fab experiment data: we found selective suppression of Ab responses to the previously immunized antigenic site but, in this protocol, also an augmented response to drifted sites (Fig. 7c). Neither approach induced detectable anti-stem titers (Supplementary Table 2). This finding helps explain the great variability observed in the phenomenon of original antigenic sin (OAS), whereby administration route, order of virus administration, and timing all play a key role in OAS induction[29].

## DISCUSSION

The ability to rationally focus vaccine-induced Ab responses onto targeted antigenic sites requires deeper understanding of Ab immunodominance, with the first step being characterization of the B cell and Ab immunodominance hierarchies. By selecting a panel of IAV escape mutants that maintain antigenicity in 1 of 5 HA globular domain antigenic sites, we could explore responses at the level of individual antigenic sites.

Dissecting GC B cell and Ab immunodominance revealed that Cb-specific B cells dominate the immediate response following infection, extending hybridoma-based findings[12,13,30]. A previous study reported that B cells expressing nearly germline Ig of a single idiotype (specific for Cb[12]) dominated early extrafollicular and later follicular B cell responses[18]. Extrafollicular B cells may account for the d 14 serum Abs to Sb-, Ca1- and Ca2-sites given the low frequency of corresponding GC B cells.

By d 21 p.i., we detect a strong Sb-specific GC B cell response. Over the next two weeks Sa- and Ca2- specific responses rise, with Ca1 responses detected only weeks later. Importantly, serum Abs and LN GC B-cell frequencies strongly correlate, suggesting that GC-originating B cells provide a substantial fraction of serum Abs, and implying that that there are little differences in the average proliferative capacities or Ab secretion rates between GC B cell progeny once they leave the LN.

We find clear differences in the immunodominance hierarchies of C57BL/6 versus BALB/c mice. The extent to which this is due to differences in Ig genes versus other genetic or epigenetic (*e.g.* microbiota) factors remains a key question that could be addressed by using the collaborative cross mice[31]. From this finding, we would predict significant differences in the immunodominance hierarchy in individual humans, no doubt enhanced by environmental factors, not least of which is the history of previous infections with IAV[32].

Importantly, the immunodominance hierarchies in infected animals versus animals immunized with inactivated virus differ significantly. After i.m. injection with adjuvant, Sa-specific Abs dominate the response at d 14 and d 28, with Sb-specific Abs making a major contribution at d 28. Following i.p. immunization, Sa and Sb-specific Abs dominate responses at d 14 and 28. Since splenic GC B cell frequencies correlate well with the serum responses, we cannot attribute these to intrinsic differences in B cell precursor frequencies, but rather the mode of antigenic delivery to the spleen. For later day responses, GCs persist far longer following infection[18,22,33,34] versus immunization[35,36], which may contribute to the time dependent diversification of responses after infection. Residual antigen presentation following i.n. infection could also contribute to continuous diversification of the repertoire specificity[37].

We confirmed previous findings that B cells can respond to IAV in the absence of T cell help, but with subdued and much more transient serum Ab responses[24,25]. We show that eliminating CD4^{+} T cells (and consequently, GCs) has little effect on the immunodominance hierarchy following either i.n. infection or i.p immunization. This is consistent with the idea that immunodominance hierarchy is initially governed by intrinsic properties of the B cell repertoire.

Analysis of pAbs induced by the 4 viruses (normalizing responses to the ELISA titers) recapitulated previous results (J. Yewdell, W. Gerhard, unpublished) that Sa-, Sb-, and Ca1-specific mAbs exert the highest VN activities, Cb the least, with Ca2 mAbs in between (Supplementary Table 3). Based on $AC_{50}$ analysis of GC B cells, this cannot be attributed to Ab affinity differences. A simple explanation for these findings is that epitope proximity to the sialic acid receptor site governs *in vitro* neutralization efficiency.

Antigenic site specific-serum HI activity mostly paralleled the VN results, with the surprise that Sb specific-Abs exhibit low specific activity, in distinct contrast to mAbs. Whatever the mechanism, this shows that site-specific differences in polyclonal functional assays may not be revealed at the level of mAbs, underscoring the importance of tackling Ab function in the natural polyclonal serum environment.

Finally, we found that upon immunogen re-challenge, Abs selectively suppress responses against the cognate antigenic site, enabling B cells specific for non-dominant sites to rise in the immunodominance hierarchy. This, is the opposite of the phenomenon of OAS, whereby immune responses are heavily skewed towards determinants shared by challenge and priming viruses[38]. It is precedented however, by recent studies showing the conditional nature of OAS[29,39] and that pre-existing human Ab levels negatively correlate with boosting responses to the same strain[40,41]. Ultimately, the strength of OAS may be governed by the

balance of Abs versus their cognate memory B cells. With high Ab levels, responses are suppressed; with low Ab levels, memory B cells dominate naïve B cells. Our findings indicate that, when using a single immunogen, responses can be focused on various domains by including the appropriate antibody or antibody like molecule[42] that sterically prevents Ab access to a given antigenic site if relevant memory cells are present.

## ONLINE METHODS

### Animals

C57BL/6 mice were purchased from Taconic Farm. For all experiments female 8–12 weeks old mice were used and randomly assigned to experimental group. All mice were held under specific pathogen-free conditions. All animal procedures were approved and performed in accordance with the NIAID Animal Care and Use Committee Guidelines.

### Virus and 4 virus selection

A/Puerto Rico/8/34 (PR8) (Mt. Sinai strain; H1N1) and mutants were grown in 10 d-old embryonated chicken eggs. Mutants were selected using MDCK-culture system as described before[15]. Hybridoma anti-HA Abs were produced as previously described[9,10,14,44]. Briefly, virus was serially diluted 10 fold in a 96-well plate. Combination of mAbs specific for one site at over-neutralizing concentration was incubated with the virus for one hour. After incubation for 2 h at 37 °C on MDCK, cells were washed and incubated with selection media in the presence of mAbs. Supernatant viral RNA from cytophatic effect-positive wells was sequenced. All the unique viruses were tested for proper escape with a large panel of mAbs. Upon satisfactory escape the mutant virus was subjected to a second round of selection with mAb of different site specificity. The procedure was repeated until 4 variants were obtained.

### Viral HA purification

Allantoic fluid was clarified by centrifugation and virus purified over sucrose gradient as described[8]. For ELISA, purified virus was fractionated by incubation with an equal volume of 15% octyl-β-glucoside. After addition of PBS the solution was spun at $50,000 \times g$ for 2 h at 4°C. The supernatant, containing HA and NA, was incubated at 56°C for 30 min after addition of 10 mM EDTA. The amount of HA in the different viral preparations was normalized using a combination of methods and confirmed by immunoblot using a $HA_2$-specific mAb (data not shown). To further confirm the accuracy of our protein estimation, serum recognition of PR8 and 4 HA was directly compared when using virus-purified HA versus rHA probes: the results were remarkably similar, confirming the validity of our estimation (Supplementary Fig. 1b).

### Infections and immunizations

For intranasal infections mice were anesthetized with isofluorane and inoculated into the nostrils with 50 $TCID_{50}$ of virus diluted in Balanced Salt Solution (BSS) 0.1% BSA. For i.p. injections the virus was UV inactivated for 4 min on ice and subsequently diluted 1:2 in sterile PBS; 2500 HA U of virus in 400 µl were injected per mouse. For i.m. immunizations 10 µg of purified virus in 25 µl PBS was UV inactivated on ice for 6 minutes; inactivated

virus was mixed with 25 μl Titermax Gold adjuvant (Sigma) and injected into the caudal thigh. For CD4^{+} T cell depletion the mAb GK1.5 was administered i.p. one day before infection or immunization and subsequently every third day. Depletion was confirmed by flow cytometry. H28-E23 Fab was pre-incubated with UV inactivated PR8 virus for 1 h at 22°C before i.p. injection.

### ELISA and serum quantification

Macrolon medium binding half-well ELISA plates (Greiner Biotech) were coated overnight at 4 °C with purified HAs in 25 μl PBS. Plates were blocked with 50 μl PBS plus 4% milk for 2 h at 22°C. After 3× washes with PBS+0.05% Tween-20 (PBST) plates were incubated with 25 μl of sera was twofold serially diluted starting from 1:100 in PBST for 1 h at 22°C. After 3× washes plates were incubated with 25 μl of rat anti-mouse kappa specific HRP-conjugated (Southern Biotech) diluted 1:1000 for 1 h at 22°C. For heavy chain determination, plates were incubated with biotinylated anti-mouse IgG/IgM followed by Avidin-D-Peroxidase incubation (VectorLab). After 3× washes plates were developed for 5 min using TMB substrate (KPL biomedical) and halted with 0.1 N HCl. Plates were read at 450 nm. ELISA binding is expressed as area under the curve (AUC) as it better captures changes both in affinity as well as maximum binding of the pAbs. Curves and AUC were determined using GraphPad Prism software.

### Hemagglutination inhibition and microneutralization

HI assay was performed in 96-well round bottom as previously described[15]. Briefly, serum was serially diluted and incubated with 4 HA U PR8 for 30 min at 22°C before adding 1% turkey RBCs for 1 h at 22°C. Microneutralization assay on MDCK cells was also performed as previously[15] with minor modifications: twofold diluted sera was incubated for 30 min at 37 °C with 100 $TCID_{50}$ of PR8 before addition to confluent MDCK cells for 1 h at 37 °C. Cells were washed and media replaced with one containing 1 μg/ml of TPCK trypsin. Cytopathic effect was assessed after 4 d.

### Flow cytometric detection of rHA-specific GC B cells

The procedure was nearly identical to the one described[22] with a few modifications. Mediastinal lymph nodes or spleens were harvested from euthanized mice at different times after infection or immunization. Single-cell suspensions were stained with the following labeled mAbs: CD3ε-PacificBlue, B220-PECy7, CD38-FITC, GL7-PE (BD Biosciences). rHA was used at 0.1 μg/ml and detected using streptavidin-APC (eBioscience). Cell viability was assessed using 10 μg/ml Ethidium Monoazide Bromide (EMA) (ThermoFisher). Samples were analyzed using a BD LSRFortessa X-20 instrument. Analysis was performed using FlowJo software (TreeStar).

### $AC_{50}$ measurement of GC B cell population affinity

Mediastinal lymph nodes were prepared and stained as above, using a low input cell number per tube ($1–2 \times 10^4$ antigen-specific cells per tube) and incubated with a graded concentration of rHA (0.66 nM to 66 nM). Data were plotted using frequency of rHA positive B cells and

50% maximal binding ($AC_{50}$) calculated using a single one-site binding with Hill slope calculation[22].

### ELISPOT detection of ASCs

PVDF plates (EMD Millipore) were activated with 35% EtOH for 5 min 22°C. After substantial washes with $dH_2O$ and PBS, wells were coated overnight at 22°C in humid chamber with 0.75 μg of goat-anti-mouse-IgG (Jackson Laboratories) in PBS.

At d 3, 7, 9, 14 and 17 mediastinal lymph nodes were excised and individually processed in a single cell suspension. Plates were blocked with PBS plus 2% BSA for 1 h at 22°C and washed with PBST and RPMI. Cells were incubated in serial twofold dilutions starting at $5 \times 10^5$ in RPMI plus 7% FCS for 18–20 h at 37 °C.

Cells were lysed with extensive $dH_2O$ washes and wells incubated with 5 ng of rHA for 2 h at 22°C. Detection was carried out after 1 h incubation with Avidin D-HRP (VectorLabs) 1:1000 by 10 minutes incubation with AEC substrate set (BD Biosciences). Spots were counted for each well with CTL ImmunoSpot analyzer and data analyzed with CTL ImmunoSpot software.

### Lymph node sectioning and germinal center staining

Mediastinal lymph nodes or spleen segments were fixed in PLP fixative (periodate-lysine-paraformaldehyde) overnight as reported previously[45], cryoprotected in 15% sucrose, embedded in OCT medium (Electron Microscopy Sciences) and frozen in dry-ice cooled isopentane. Sixteen-micron sections were cut on a Leica cryostat (Leica Microsystems), blocked with 5% goat or donkey serum then stained with a combination of the following: B220 (clone RA3-6B2), GL-7 (clone GL-7), CD38 (clone RP-T8) and detected using fluorescent secondary antibodies (ThermoFisher Scientific). Sections were incubated with secondary antibodies only as controls, and images were acquired using identical PMT (photomultiplier tube) and laser settings using a Leica SP5 confocal microscope.

### Statistical analysis

AUC and all curves were calculated using one site binding with Hill slope curve fitting. Correlation was assessed using the Pearson correlation coefficient. Sample size for animal studies was based on previous experience. Animal studies were performed without blinding. One-way ANOVA with post-hoc Tukey's multiple comparison test was applied when indicated in the figure legend. All were determined using GraphPad Prism (GraphPad Software Inc.).

## Supplementary Material

Refer to Web version on PubMed Central for supplementary material.

## Acknowledgments

# References

1. Yewdell JW. Confronting complexity: real-world immunodominance in antiviral CD8+ T cell responses. Immunity. 2006; 25:533–543. [PubMed: 17046682]

2. Krammer F, Palese P. Advances in the development of influenza virus vaccines. Nat Rev Drug Discov. 2015; 14:167–182. [PubMed: 25722244]

3. Burton DR, Poignard P, Stanfield RL, Wilson IA. Broadly neutralizing antibodies present new prospects to counter highly antigenically diverse viruses. Science. 2012; 337:183–186. [PubMed: 22798606]

4. Wheatley AK, Kent SJ. Prospects for antibody-based universal influenza vaccines in the context of widespread pre-existing immunity. Expert Rev Vaccines. 2015; 14:1227–1239. [PubMed: 26175180]

5. Victora GD, Wilson PC. Germinal Center Selection and the Antibody Response to Influenza. Cell. 2015; 163:545–548. [PubMed: 26496601]

6. Hutchinson EC, et al. Conserved and host-specific features of influenza virion architecture. Nature communications. 2014; 5:4816.

7. Reading SA, Dimmock NJ. Neutralization of animal virus infectivity by antibody. Arch Virol. 2007; 152:1047–1059. [PubMed: 17516034]

8. Altman MO, Bennink JR, Yewdell JW, Herrin BR. Lamprey VLRB response to influenza virus supports universal rules of immunogenicity and antigenicity. Elife. 2015; 4

9. Caton AJ, Brownlee GG, Yewdell JW, Gerhard W. The antigenic structure of the influenza virus A/PR/8/34 hemagglutinin (H1 subtype). Cell. 1982; 31:417–427. [PubMed: 6186384]

10. Gerhard W, Yewdell J, Frankel ME, Webster R. Antigenic structure of influenza virus haemagglutinin defined by hybridoma antibodies. Nature. 1981; 290:713–717. [PubMed: 6163993]

11. Yewdell JW, Webster RG, Gerhard WU. Antigenic variation in three distinct determinants of an influenza type A haemagglutinin molecule. Nature. 1979; 279:246–248. [PubMed: 86955]

12. Kavaler J, Caton AJ, Staudt LM, Schwartz D, Gerhard W. A set of closely related antibodies dominates the primary antibody response to the antigenic site CB of the A/PR/8/34 influenza virus hemagglutinin. Journal of immunology (Baltimore, Md. : 1950). 1990; 145:2312–2321.

13. McKean D, et al. Generation of antibody diversity in the immune response of BALB/c mice to influenza virus hemagglutinin. Proc Natl Acad Sci U S A. 1984; 81:3180–3184. [PubMed: 6203114]

14. Staudt LM, Gerhard W. Generation of antibody diversity in the immune response of BALB/c mice to influenza virus hemagglutinin. I. Significant variation in repertoire expression between individual mice. J Exp Med. 1983; 157:687–704. [PubMed: 6600489]

15. Das SR, et al. Defining influenza A virus hemagglutinin antigenic drift by sequential monoclonal antibody selection. Cell Host Microbe. 2013; 13:314–323. [PubMed: 23498956]

16. Lubeck M, Gerhard W. Conformational changes at topologically distinct antigenic sites on the influenza A/PR/8/34 virus HA molecule are induced by the binding of monoclonal antibodies. Virology. 1982; 118:1–7. [PubMed: 6177092]

17. Marshall D, Sealy R, Sangster M, Coleclough C. TH cells primed during influenza virus infection provide help for qualitatively distinct antibody responses to subsequent immunization. Journal of immunology (Baltimore, Md. : 1950). 1999; 163:4673–4682.

18. Rothaeusler K, Baumgarth N. B-cell fate decisions following influenza virus infection. European journal of immunology. 2010; 40:366–377. [PubMed: 19946883]

19. Sealy R, Surman S, Hurwitz JL, Coleclough C. Antibody response to influenza infection of mice: different patterns for glycoprotein and nucleocapsid antigens. Immunology. 2003; 108:431–439. [PubMed: 12667204]

20. Baumgarth N. How specific is too specific? B-cell responses to viral infections reveal the importance of breadth over depth. Immunological reviews. 2013; 255:82–94. [PubMed: 23947349]

21. Whittle JR, et al. Flow cytometry reveals that H5N1 vaccination elicits cross-reactive stem-directed antibodies from multiple Ig heavy-chain lineages. J Virol. 2014; 88:4047–4057. [PubMed: 24501410]

22. Frank GM, et al. A Simple Flow-Cytometric Method Measuring B Cell Surface Immunoglobulin Avidity Enables Characterization of Affinity Maturation to Influenza A Virus. MBio. 2015; 6:e01156. [PubMed: 26242629]

23. Tsilibary EC, Wissig SL. Light and electron microscope observations of the lymphatic drainage units of the peritoneal cavity of rodents. Am J Anat. 1987; 180:195–207. [PubMed: 2445193]

24. Lee BO, et al. CD4 T cell-independent antibody response promotes resolution of primary influenza infection and helps to prevent reinfection. Journal of immunology (Baltimore, Md. : 1950). 2005; 175:5827–5838.

25. Mozdzanowska K, Furchner M, Zharikova D, Feng J, Gerhard W. Roles of CD4+ T-cell-independent and -dependent antibody responses in the control of influenza virus infection: evidence for noncognate CD4+ T-cell activities that enhance the therapeutic activity of antiviral antibodies. J Virol. 2005; 79:5943–5951. [PubMed: 15857980]

26. Hai R, et al. Influenza viruses expressing chimeric hemagglutinins: globular head and stalk domains derived from different subtypes. J Virol. 2012; 86:5774–5781. [PubMed: 22398287]

27. Bennink JR, Doherty PC. The response to H-2-different virus-infected cells is mediated by long-lived T lymphocytes and is diminished by prior virus priming in a syngeneic environment. Cell Immunol. 1981; 61:220–224. [PubMed: 6973400]

28. Jamieson BD, Ahmed R. T cell memory. Long-term persistence of virus-specific cytotoxic T cells. J Exp Med. 1989; 169:1993–2005. [PubMed: 2471771]

29. Kim JH, Skountzou I, Compans R, Jacob J. Original antigenic sin responses to influenza viruses. Journal of immunology (Baltimore, Md. : 1950). 2009; 183:3294–3301.

30. Kavaler J, Caton AJ, Staudt LM, Gerhard W. A B cell population that dominates the primary response to influenza virus hemagglutinin does not participate in the memory response. European journal of immunology. 1991; 21:2687–2695. [PubMed: 1936117]

31. Churchill GA, et al. The Collaborative Cross, a community resource for the genetic analysis of complex traits. Nat Genet. 2004; 36:1133–1137. [PubMed: 15514660]

32. Linderman SL, et al. Potential antigenic explanation for atypical H1N1 infections among middle-aged adults during the 2013–2014 influenza season. Proc Natl Acad Sci U S A. 2014; 111:15798–15803. [PubMed: 25331901]

33. Jelley-Gibbs DM, et al. Unexpected prolonged presentation of influenza antigens promotes CD4 T cell memory generation. The Journal of Experimental Medicine. 2005; 202:697–706. [PubMed: 16147980]

34. Waffarn EE, Baumgarth N. Protective B cell responses to flu--no fluke! Journal of immunology (Baltimore, Md. : 1950). 2011; 186:3823–3829.

35. MacLennan ICM. Germinal centers. Annual Review of Immunology. 1994; 12:117–139.

36. Hollowood K, Macartney J. Cell kinetics of the germinal center reaction--a stathmokinetic study. European journal of immunology. 1992; 22:261–266. [PubMed: 1730253]

37. Zammit DJ, Turner DL, Klonowski KD, Lefrancois L, Cauley LS. Residual antigen presentation after influenza virus infection affects CD8 T cell activation and migration. Immunity. 2006; 24:439–449. [PubMed: 16618602]

38. Fazekas de St. Groth S, Webster RG. Disquisition on original antigenic sin. I. Evidence in man. Journal of Experimental Medicine. 1966; 124:331–345. [PubMed: 5922742]

39. Kim JH, Davis WG, Sambhara S, Jacob J. Strategies to alleviate original antigenic sin responses to influenza viruses. Proc Natl Acad Sci U S A. 2012; 109:13751–13756. [PubMed: 22869731]

40. Andrews SF, et al. High preexisting serological antibody levels correlate with diversification of the influenza vaccine response. J Virol. 2015; 89:3308–3317. [PubMed: 25589639]

41. Sasaki S, et al. Influence of prior influenza vaccination on antibody and B-cell responses. PloS one. 2008; 3:e2975. [PubMed: 18714352]

42. Fleishman SJ, et al. Computational design of proteins targeting the conserved stem region of influenza hemagglutinin. Science. 2011; 332:816–821. [PubMed: 21566186]

43. Gamblin SJ, et al. The structure and receptor binding properties of the 1918 influenza hemagglutinin. Science. 2004; 303:1838–1842. [PubMed: 14764886]

## METHODS ONLY REFERENCES

44. Yewdell JW, Gerhard W. Antigenic characterization of viruses by monoclonal antibodies. Annual Review of Microbiology. 1981; 35:185–206.

45. Pieri L, Sassoli C, Romagnoli P, Domenici L. Use of periodate-lysine-paraformaldehyde for the fixation of multiple antigens in human skin biopsies. Eur J Histochem. 2002; 46:365–375. [PubMed: 12597622]
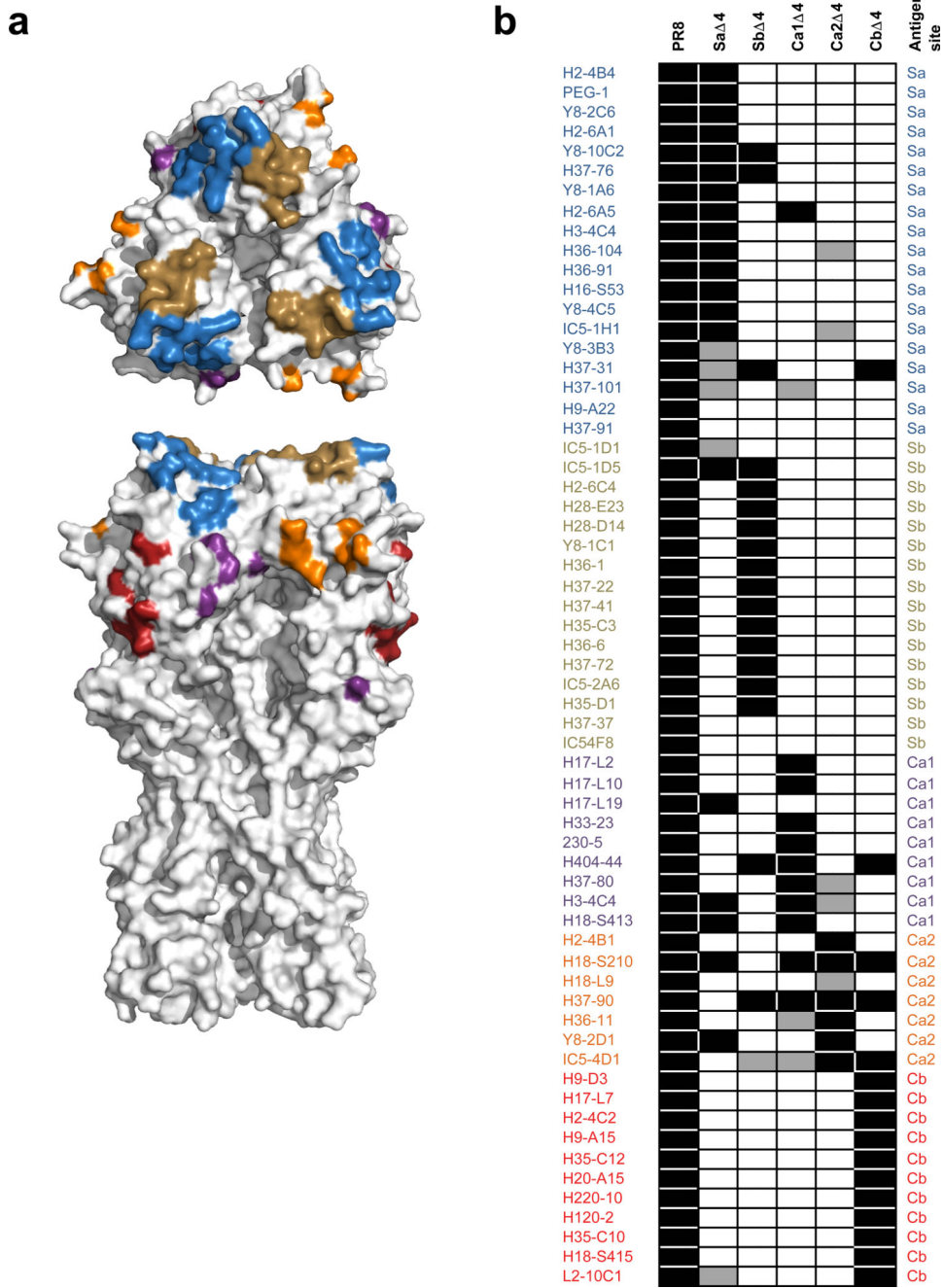
**Figure 1. Characterization of Δ4 viruses**

(**a**) Crystal structure of PR8 HA (PDB: 1RUZ[43]) viewed from top and side with the five major globular domain antigenic sites in color Sa (blue), Sb (gold), Ca1 (purple), Ca2 (orange), Cb (red). (**b**) Antigenicity of the Δ4 viruses assessed by measuring the relative binding affinity by ELISA with a panel of 62 well characterized mAbs. Black: similar affinity to the parental PR8 virus, grey: >2 but <10 fold $K_D$ reduction, white: >10fold reduction in $K_D$.
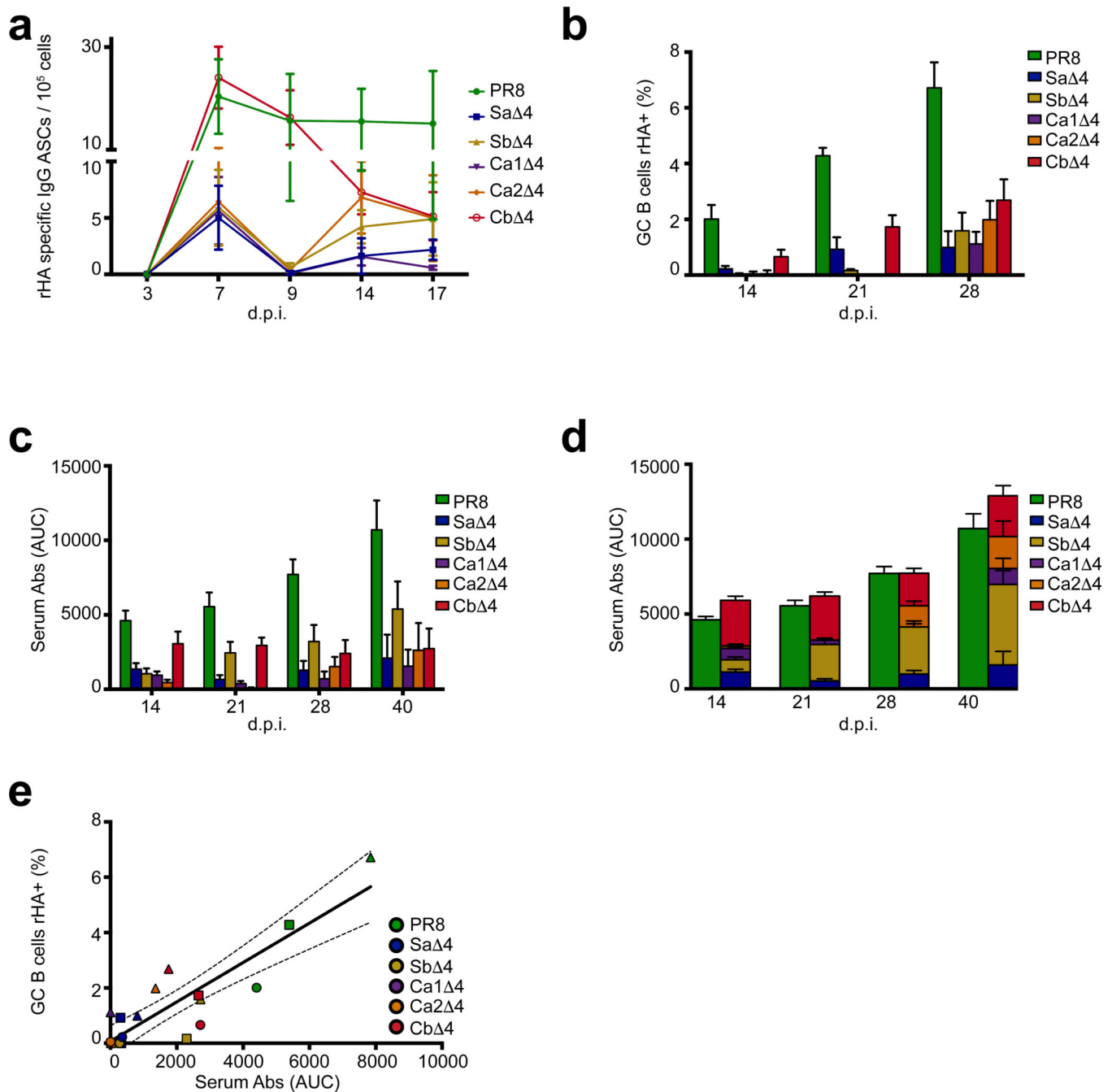
**Figure 2. B cell kinetics and Ab immunodominance upon IAV infection**

We infected C57BL/6 mice i.n. with 50 $TCID_{50}$ PR8. (**a**) At the indicated time points MLN were collected and analyzed individually by ELISPOT on rHA derived from the different viruses. Graph represent mean and s.e.m. (bars) of three independent experiments with 3 individual mice each. (**b**) Bar graph showing the frequency of antigenic site-specific germinal center B cells at different d.p.i.. Column represent mean and SEM (bars). S12 frequencies were considered baseline and subtracted from PR8 and Δ4 values. Shown are three independent experiments where MLN from 5 animals were pooled. (**c**) We tested

serum collected 14, 21, 28, 40 d.p.i. by ELISA for recognition of PR8, 4 HAs. S12 AUC were considered baseline and subtracted from PR8 and 4 values. Graph represents mean and bars SEM of two independent experiments with 5 mice each. (**d**) Bar graph showing cumulative serum Abs response. After S12 AUC subtraction, the sum of the response to the 5 antigenic sites is close to equal to the PR8 response. Columns represent means and SEM (bars). (**e**) Scatter plot showing the correlation between ELISA recognition of the different HAs (as in **c**) and frequency of GC B cells (as in **b**). *P*<0.0001 *r*=0.8814. Circles represent 14 d p.i., squares 21 d p.i. and triangles 28 d p.i.. Dashed lines represent 95% confidence intervals.
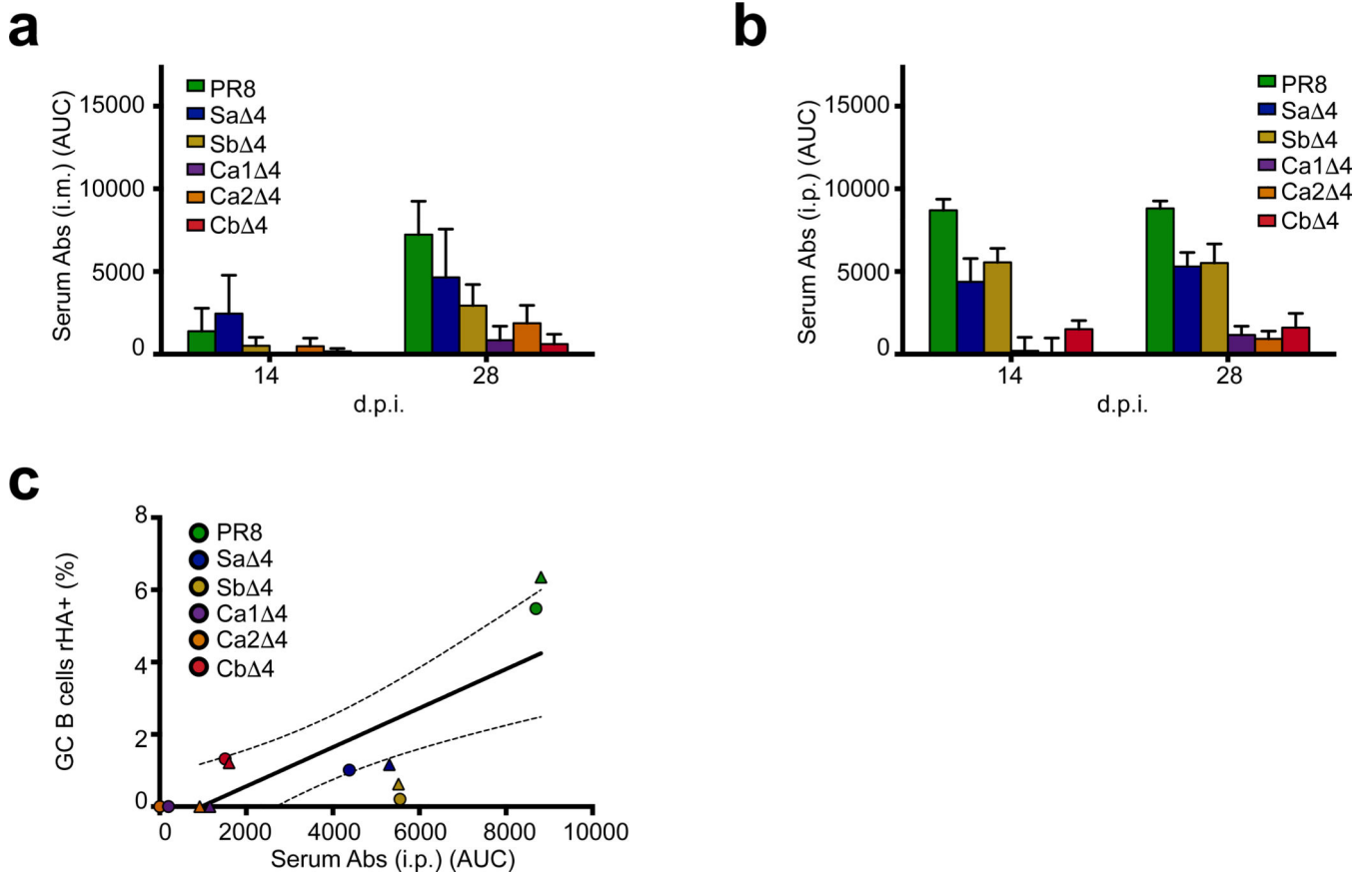
**Figure 3. Intraperitoneal and intramuscular immunizations elicit similar Ab immunodominance patterns distinct from infection**

We immunized mice i.m with 6µg of UV-inactivated virus with Titermax adjuvant (**a**) or i.p. with 2500HAU of UV-inactivated-PR8 (**b**). We assayed serum collected 14 and 28 d p.i by ELISA for recognition of PR8 and 4 HAs. S12 AUC were considered baseline and subtracted from PR8 and 4 values. Graph represents mean and SEM (bars) of two independent experiments with 3 (**a**) or 4 mice (**b**) each. (**c**) Scatter plot shows correlation between the frequency of splenic GC B cells and ELISA recognition of the different HAs (as in **b**). Shown is the average from three independent experiments where three spleens were pooled. *P*=0.0021 *r*=0.7926. Circles are 14dpi, and triangles 28dpi. Dashed lines represent 95% confidence intervals.
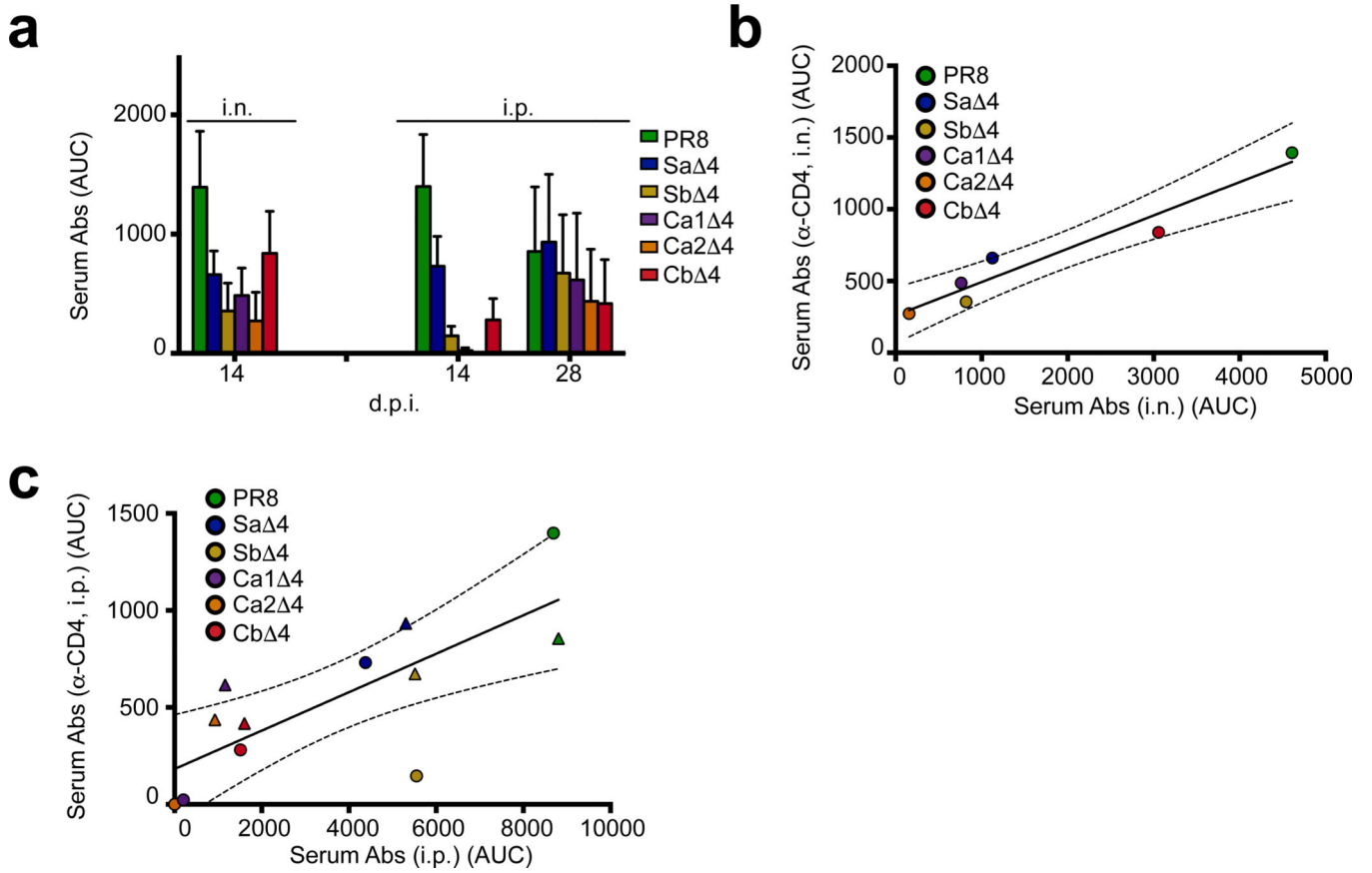
**Figure 4. CD4^{+} T cells positively modulate the magnitude and duration of Ab responses but not their immunodominance**

We depleted CD4^{+} T cells by injecting GK1.5 mAb i.p. one d before infection/ immunization, and subsequently every third day. We challenged mice by i.n. infection with 50 TCID$_{50}$ of PR8 or i.p. injection with 2500 HAU of UV-inactivated-PR8. (**a**) We collected serum 14 and 28 d p.i. and tested by ELISA for recognition of PR8, 4 and S12 HAs. S12 AUCs were considered baseline and subtracted from PR8 and 4 values. Columns represent mean and SEM (bars). Two independent experiment of 5 mice each.

(**b, c**) Scatter plot shows correlation between serum ELISA recognition of the different HAs in regular mice (as in Fig. 2c and 3b) versus CD4-depleted mice. *P*=0.0039 *r*=0.7623. Circles represent 14 d p.i., and triangles 28 d p.i.. Dashed lines represent 95% confidence intervals.
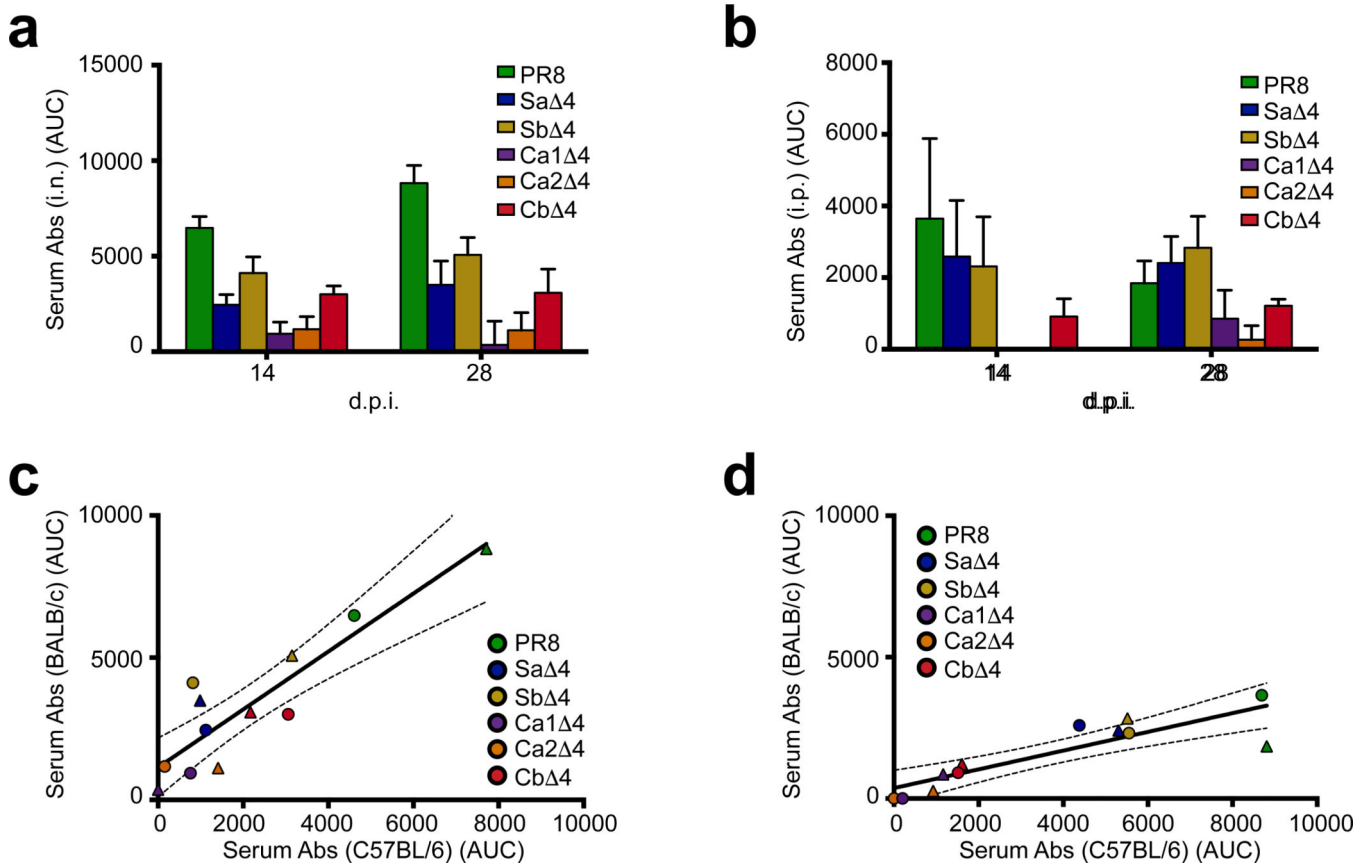
**Figure 5. Ab immunodominance varies between mouse strains**

We infected BALB/c mice i.n. with 50 $TCID_{50}$ PR8 (**a**) or injected i.p. with 2500HAU of UV-inactivated-PR8 (**b**). We collected serum at 14 and 28 d p.i. and tested by ELISA for recognition of PR8, Δ4 HAs. S12 AUCs were considered baseline and subtracted from PR8 and Δ4 values Graph represents mean and SEM (bars) of two independent experiments with 4 (**a**) or 3 (**b**) mice each. (**c**) Scatter plot showing the correlation between ELISA recognition of the different HAs in C57BL/6 (as in Fig. 2c) and BALB/c mice (as in **a**) upon i.n. infection. $P$=0.0001 $r$=0.9027. (**d**) Scatter plot showing the correlation between ELISA recognition of the different HAs in C57BL/6 (as in Fig. 3b) and BALB/c mice (as in **b**) upon i.p. immunization. $P$=0.0002 $r$=0.8684. Circles represent 14 d p.i., and triangles 28 d p.i.. Dashed lines represent 95% confidence intervals.
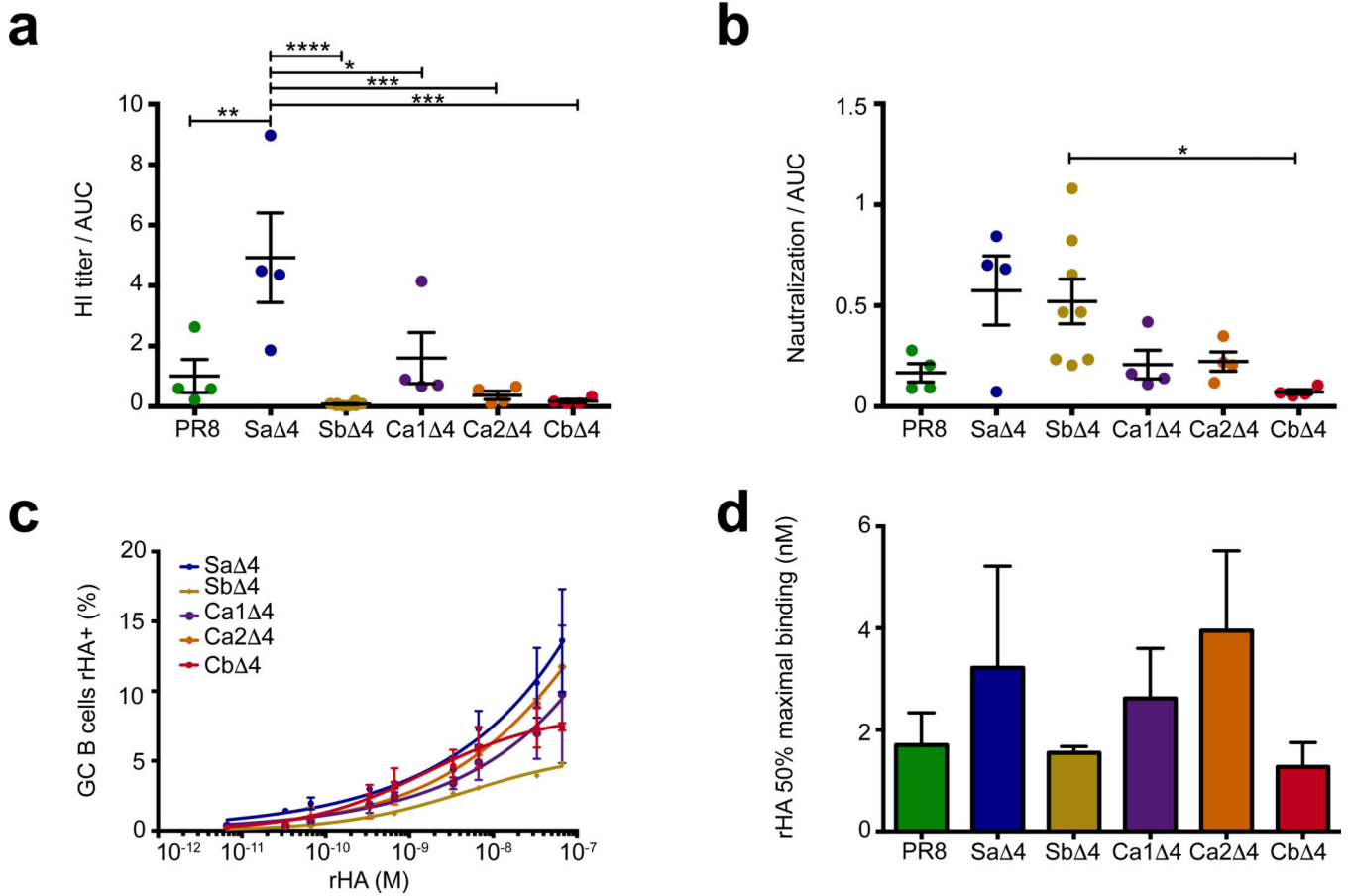
**Figure 6. Abs directed to different antigenic sites exhibit distinct functionalities**

We infected mice i.n. with 50 $TCID_{50}$ of either PR8, $\Delta 4$ virus or S12, and collected sera and MLN 21 d.p.i. for HI (**a**) and MN (**b**). Data are presented as a ratio between the HI or MN endpoint titer and the ELISA reactivity towards PR8 HA (not shown). Higher values represent higher serum efficacy. Line represent mean and SEM (bars). One-way ANOVA with post-hoc Tukey's multiple comparison (p=0.0002 for **a** and p=0.012 for **b**) (n=4 for PR8, Sa, Ca1, Ca2; n=5 for Cb and n=8 for Sb) * p<0.05, **p<0.01, ***p<0.001, ****p<0.0001. (**c**) Titration curves of MLN GC B cells to rHA$^{PR8}$ following i.n. infection with $\Delta 4$ viruses. rHA concentration (nM) necessary to reach 50% of the maximal binding was calculated for each titration curve (**d**). Line represent mean and SEM (bars). Data are from two independent experiments with pooled MLN from 5 mice each.
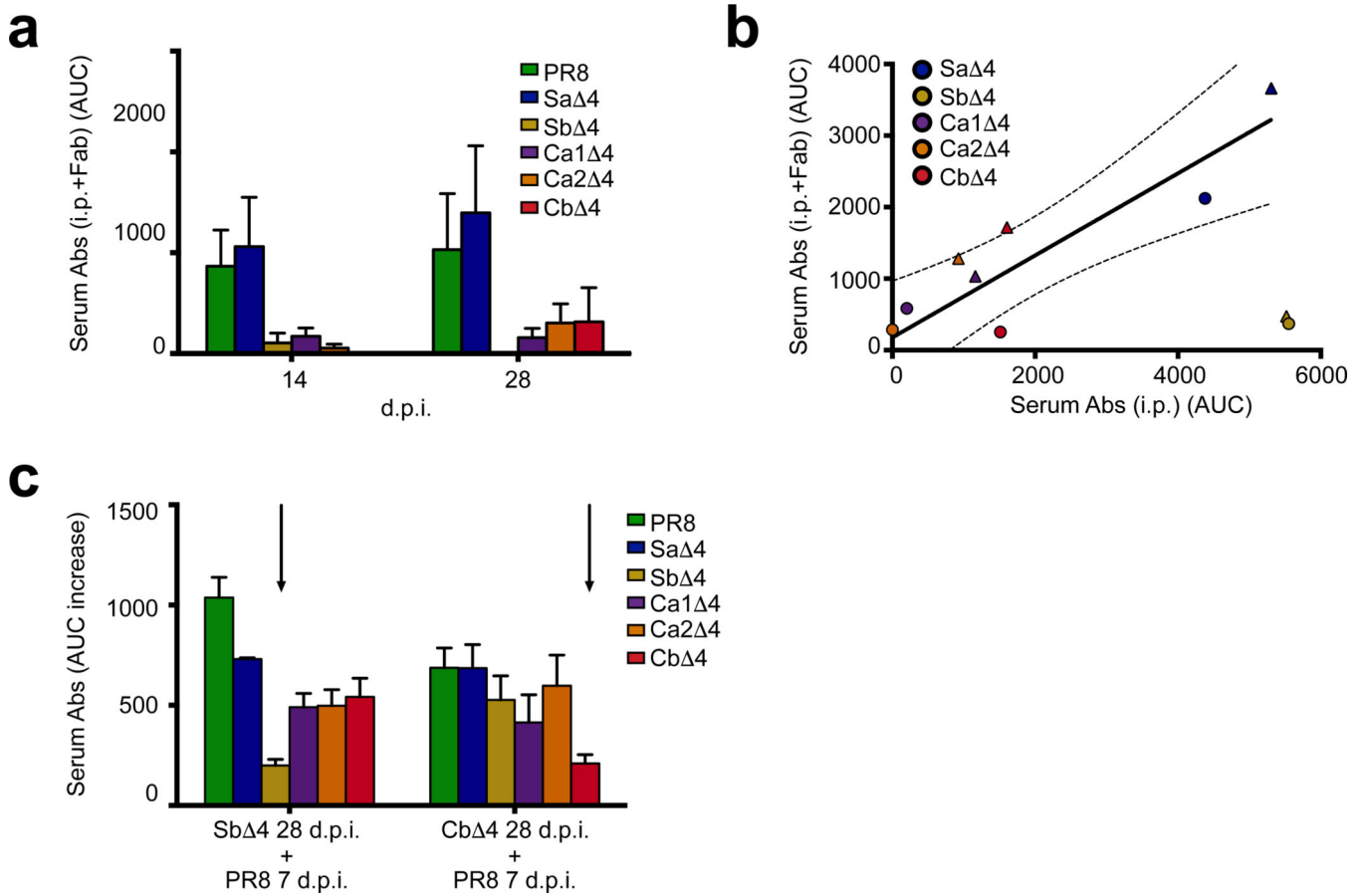
**Figure 7. Pre-existing Abs influence immunodominance of recall responses**

We immunized mice were i.p. with 2500HAU of UV-inactivated-PR8 premixed with Fabs from H28-E23, a Sb-site mAb. (**a**) We collected serum 1 d.p.i to assess the baseline Ab level and subsequently at 14 and 28 d.p.i and tested by ELISA for recognition of PR8, Δ4 and S12 -HAs. Presented are results after d 1 baseline Ab subtraction. S12 AUCs were considered baseline and subtracted from PR8 and Δ4 values. Columns represent mean and SEM (bars). Results are three technical replicates from five individual mice for each time point. (**b**) Scatter plot shows correlation between serum ELISA recognition of the different HAs after i.p. (as in Fig. 3b) versus virus+Fab i.p.. Aside from PR8 and Sb-specific responses, the general immunodominance pattern is maintained. *P*=0.0036 *r*=0.8684 are calculated excluding the Sb points. Circles represent 14 d p.i., and triangles 28 d p.i.. Dashed lines represent 95% confidence intervals. (**c**) We infected mice i.n. with 50 TCID$_{50}$ Δ4Sb or Δ4Cb virus and challenged at 28 d.p.i. i.p. with 2000 HAU of PR8. We collected sera 7 d post challenge and tested by ELISA for recognition of PR8, Δ4 and S12 HAs. Shown is the AUC after subtracting the 28 d p.i. response. Arrows indicate the site corresponding to the primary virus. Data on graph represent mean and SEM (bars) of two independent experiments with 3 mice each.